

# The Miocene Costa Giardini diatreme, Iblean Mountains, southern Italy: model for maar-diatreme formation on a submerged carbonate platform

Sonia Calvari · Lawrence H. Tanner

Received: 27 June 2009 / Accepted: 1 November 2010  
© Springer-Verlag 2010

**Abstract** In this paper we present a model for the growth of a maar-diatreme complex in a shallow marine environment. The Miocene-age Costa Giardini diatreme near Sortino, in the region of the Iblei Mountains of southern Sicily, has an outer tuff ring formed by the accumulation of debris flows and surge deposits during hydromagmatic eruptions. Vesicular lava clasts, accretionary lapilli and bombs in the older ejecta indicate that initial eruptions were of gas-rich magma. Abundant xenoliths in the upper, late-deposited beds of the ring suggest rapid magma ascent, and deepening of the eruptive vent is shown by the change in slope of the country rock. The interior of the diatreme contains nonbedded breccia composed of both volcanic and country rock clasts of variable size and amount. The occurrence of bedded hyaloclastite breccia in an isolated outcrop in the middle-lower part of the diatreme suggests subaqueous effusion at a low rate following the end of explosive activity. Intrusions of nonvesicular magma, forming plugs and dikes, occur on the western side of the diatreme, and at the margins, close to the contact between breccia deposits and country rock; they indicate involvement of volatile-poor magma, possibly during late stages of activity. We propose that initial hydromagmatic explosive

activity occurred in a shallow marine environment and the ejecta created a rampart that isolated for a short time the inner crater from the surrounding marine environment. This allowed explosive activity to draw down the water table in the vicinity of the vent and caused deepening of the explosive center. A subsequent decrease in the effusion rate and cessation of explosive eruptions allowed the crater to refill with water, at which time the hyaloclastite was deposited. Emplacement of dikes and plugs occurred nonexplosively while the breccia sediment was mostly still soft and unconsolidated, locally forming peperites. The sheltered, low-energy lagoon filled with marine limestones mixed with volcanoclastic material eroded from the surrounding ramparts. Ultimately, lagoonal sediments accumulated in the crater until subsidence or erosion of the tuff ring caused a return to normal shallow marine conditions.

**Keywords** Maar · Diatreme · Accretionary lapilli · Hyaloclastite · Volcanoclastic

## Introduction

Diatreme formation in the Iblean Mountains on eastern Sicily has long been recognised (Carbone and Lentini 1981), but apart from the recent work of Suiting and Schmincke (2009), no detailed studies on the specific processes and environment of the diatremes' formation have been published. In this paper, we present the results of detailed geological surveys conducted at the Costa Giardini Diatreme near Sortino, in the Iblean Mountains, and previously published in only limited form (Calvari and Tanner 2000). We describe the lithostratigraphic units that are evident in the field, discuss their spatial and temporal relationships, interpret the processes of their formation and

---

Editorial responsibility: J.D.L. White

S. Calvari (✉)  
Istituto Nazionale di Geofisica e Vulcanologia, sezione di Catania,  
Piazza Roma 2,  
95123 Catania, Italy  
e-mail: sonia.calvari@ct.ingv.it

L. H. Tanner  
Center for the Study of Environmental Change, Department of  
Biological Sciences, Le Moyne College,  
Syracuse, NY 13214, USA

propose a model for the emplacement and growth of the diatreme that integrates these observations.

Most authors now refer to broad, shallow craters surrounded by low rims of tephra variously as tuff rings and maars, with the former typically considered as strictly constructional features, while the latter are distinguished as features excavated into country rock (Fisher and Schmincke 1984; Lorenz 1986; Cas and Wright 1988; Aranda-Gómez and Luhr 1996; Németh et al. 2008). Maars are further distinguished by the common subsidence of the crater floor into the underlying, explosively deepened diatreme (Lorenz 1973, 1986, 2007; White 1991; Lorenz et al. 2002).

The various models for the formation of maar-diatreme complexes have been reviewed in the literature numerous times. As presented recently by Lorenz and Kurszlaukis (2007), there exist two contrasting models to explain their emplacement. The magmatic model is mainly invoked by petrologists, who attribute the driving force for diatreme formation to the explosive behaviour of carbonatite and kimberlitic magmas, a consequence of their high primary volatile content (e.g. Dawson 1980; Stoppa and Principe 1997; Skinner and Marsh 2004; Wilson and Head 2007). Alternatively, the phreatomagmatic model, now accepted by many volcanologists, attributes the common pipe conduit features to the explosive interaction between ground water and rising magma (e.g. Self et al. 1980; Lorenz 1973, 1985, 1986; Sohn et al. 2002; Lorenz 2007; Lorenz and Kurszlaukis 2007). As recently reviewed by Kurszlaukis and Lorenz (2008), the rise of low-viscosity magmas involves transport from a high to a low pressure environment, and so provides insufficient energy for large, volatile-driven explosions. In the phreatomagmatic model, the transfer of thermal energy to groundwater causes thermohydraulic explosions responsible for fragmentation and transport in expanding steam. According to Lorenz and Kurszlaukis (2007), the depth of these explosions is constrained by a pressure barrier of 2 to 3 MPa, and so the explosions occur initially at low hydrostatic pressures equivalent to depths of only tens to a few hundred meters.

Lorenz (1986, 2007) proposed a general model for the formation and evolution of maar-diatremes that relates gradual enlargement of the maar to progressive deepening and widening of the pipe conduit during the course of eruptive activity. These structures thus form by many individual phreatomagmatic explosive eruptions and associated collapse processes. As thermal energy is transferred from magma to the vaporization of groundwater, continued magma rise results in a rate of groundwater loss, as steam, that exceeds the rate of recharge of the aquifer surrounding the explosive centre (Kurszlaukis and Lorenz 2008). Hence, a cone of depression forms in the local water table resulting in an increase of the depth of the hydrostatic pressure barrier. Consequently, rising magma will interact explo-

sively with groundwater at greater depth and create explosion chambers deeper in the root zone (Kurszlaukis and Lorenz 2008). Spalling of wall rock surrounding the conduit, fractured by the shock waves from the explosions, causes the collapse of the sides of the maar along many inward-dipping failure surfaces, resulting in the characteristic funnel-shaped pipe filled by a breccia consisting of fragmented volcanic products and milled country rock.

Maar-diatreme complexes became well-known first through the study of diamond-bearing kimberlite pipes in hard-rock continental settings such as the South African kimberlite pipes (see review in Lorenz and Kurszlaukis 2007). More recently, attention has been directed towards their formation in sedimentary environments, particularly soft-sediment environments, where the explosive force is presumably provided by magma-groundwater interactions (see Lorenz 1973, 1985, 1986; Boxer et al. 1989; White 1991, 1996, 2000; Lorenz et al. 2002). Well-known examples of diatremes formed within soft sediments include the Missouri River Breaks (Hearn 1968). Lorenz (1986) considered the formation of maar-diatreme complexes unlikely in subaqueous environments due to the ready availability of water at the surface, preventing deepening of the explosive centre. Nevertheless, examples exist of maar-diatreme complexes formed by eruptions that began subaqueously in lacustrine settings, such as the Table Rock Maar (Brand and Clarke 2009). Lefebvre and Kurszlaukis (2008) interpreted a Cretaceous kimberlite in Saskatchewan as having formed within country rock, but in a submarine environment in which the formation of a tephra ring restricted the access of seawater to the maar crater, and allowed deepening of the phreatomagmatic explosions in the root zone.

There are, however, only a few reports on any type of explosive volcanic activity in active carbonate-forming environments. Martin et al. (2004) interpreted drill cores of interbedded volcanoclastic rocks and carbonates of Cretaceous age from a guyot in the West Pacific as evidence for the excavation of a broad crater by explosive eruptions in semi-consolidated platform carbonates. In their model, however, the feature remained entirely submerged, and lacked a surrounding tuff ring or underlying diatreme. More recently, Basile and Chauvet (2009) described the formation of a maar-like feature on an active carbonate platform of Triassic age, but here also, the authors infer that the eruption neither deepened the explosive center nor formed a surrounding tuff ring. The morphology and vertical and lateral distribution of lithostratigraphic units that we describe in the Costa Giardini, near Sortino, Sicily, provide evidence for the formation of a maar-diatreme complex on a submerged carbonate platform during the Late Miocene (Turtonian). We suggest that this emplace-

ment model may also be applicable to other pipes or conduits that have been assumed to form in strictly subaerial settings.

## Geologic setting

The complex geodynamic environment of southern Italy is controlled by the tectonics of collision between Africa and Europe, ongoing since the Middle Miocene. Most of the southern part of the island of Sicily, in southern Italy, represents the northern edge of the African plate (Fig. 1), whereas the northernmost corner of Sicily is part of the Apennine-Maghrebian Chain on the Eurasian plate (Barberi et al. 1974; Catalano et al. 1996). The Iblean Plateau occupies the south-east corner of Sicily, and is a stable carbonate foreland separated from the thrust zones to the north by the Gela-Catania foredeep (Grasso et al. 1983). The Iblean Plateau is divided from the Ionian Abyssal Plain by the faults of the Ibleo-Maltese Escarpment (Fig. 1). During the Neogene this area has been the centre for widespread volcanic activity and associated uplift, alternating with several phases of subsidence, with the progressive consumption of the northern margin of the Iblean plateau leading to the development of the modern foredeep (Yellin-Dror et al. 1997). The Iblean plateau is transected by predominantly post-depositional normal faults trending NE and NW (Pedley and Grasso 1991).

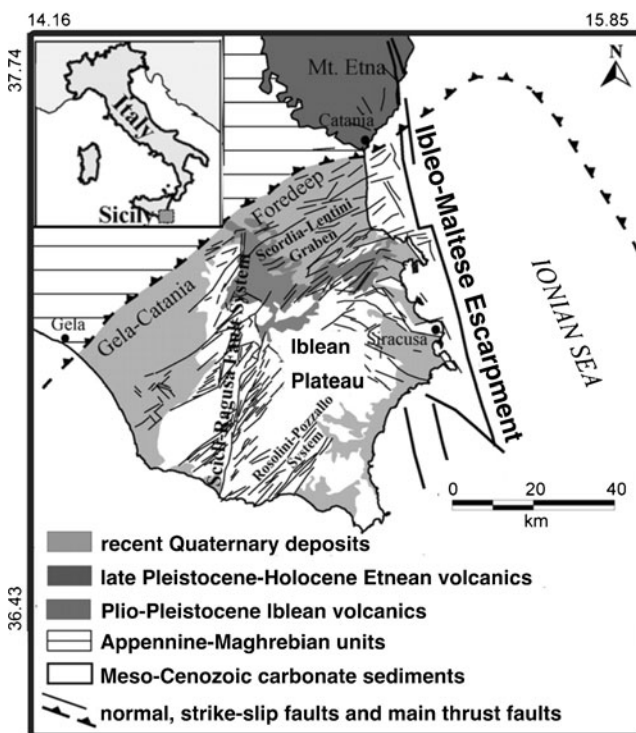
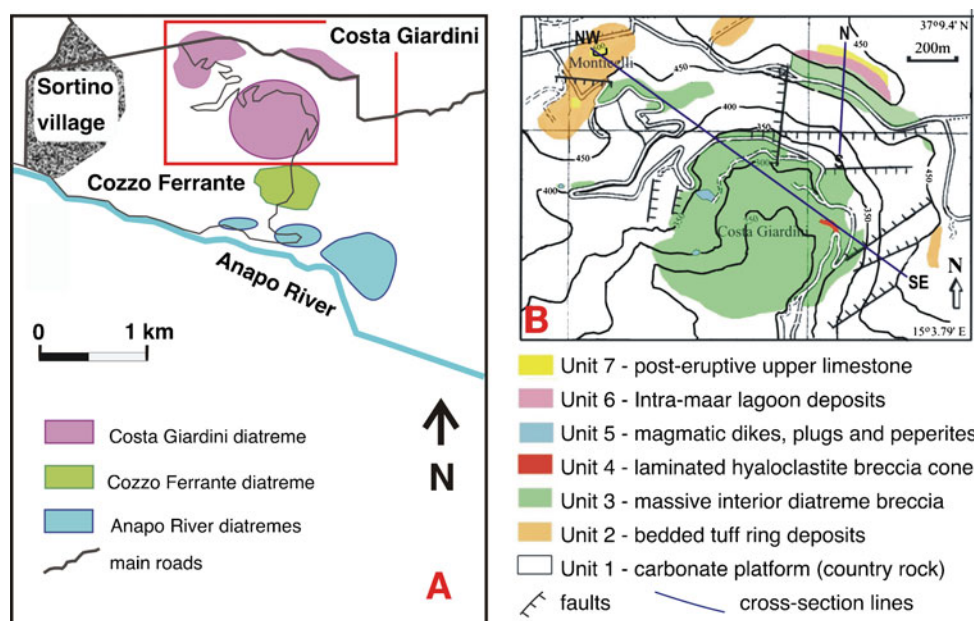


**Fig. 1** Simplified sketch map of the main structural elements of Sicily and of the Iblean plateau (modified after Scarfi et al. 2007)

Volcanic activity in this region occurred essentially in three main phases: the Upper Cretaceous, the Upper Miocene (mainly Upper Tortonian) and the Pliocene (Grasso et al. 1983). The late Miocene to Pleistocene volcanic rocks were emplaced both in submarine and subaerial environments on a platform that varied between shallow submerged and emergent conditions, due to uplift, and sea-level changes that accompanied both sedimentation and volcanism (Schmincke et al. 1997). In the eastern part of the Iblean Plateau, the Miocene volcanic and volcanoclastic rocks display both a tholeiitic and Na-alkaline affinity (Tonarini et al. 1996; Schmincke et al. 1997) and occur within a shallow marine sequence assigned to the Carlentini Formation (CF) by Grasso et al. (1982, 1983). As described at the type section by Grasso et al. (1982), the CF sequence rests on the brecciated Siracusa Limestone Member of the Monte Climiti Formation, and is covered by the (mostly Messinian) Monte Carrubba Formation, which consists predominantly of micritic carbonates and subordinate grainstones. These formations are all part of the Sortino Group, which is in turn overlain by Pliocene lava flows. At the type location, the CF comprises 45 m of mainly volcanoclastic deposits, consisting of tuff and agglomerates, interbedded with several subordinate m-scale carbonate beds, including two bioherm units. The relationship of most of the volcanic rocks in the CF to explosion pipe conduits was recognised long ago (Carbone and Lentini 1981), but no detailed studies on these sequences and the mechanisms of their origin have been conducted until recently.

The volcanoclastic sequence near Sortino described in this paper is related to a single diatreme feeder vent and is more than 265 m thick (Fig. 2a, b), which is substantially greater than the type thickness of the CF as described by Grasso et al. (1982). However, we follow the usage of previous authors that refer the whole of the sequence to the CF. Carbone and Lentini (1981) mapped eleven diatreme conduits within the CF in an area of ~207 km<sup>2</sup> surrounding Sortino, and immediately east of Sortino they recognised the pipe conduit at Costa Giardini. In our reconnaissance survey of an area of slightly less than 10 km<sup>2</sup> surrounding Sortino, we recognised five distinctive diatreme conduits with at least partial exposure (Fig. 2a). Of these, the largest and best exposed is the Costa Giardini diatreme (CGD), originally mapped by Carbone and Lentini (1981). Calvari and Tanner (2000) first described this feature as a pipe-conduit complex developed specifically in a submarine setting. Many of the prominent features of the CGD were described subsequently in a field-trip guidebook (Schmincke et al. 2004), and most recently Suiting and Schmincke (2009) proposed a model for formation of the CGD invoking rapid ascent of a high-volatile magma (the magmatic model described above). In this paper we further describe the volcanic features of this structure and propose as an

**Fig. 2** (a) Geologic sketch map of the diatremes exposed east of Sortino village in the Iblean Mountains, southern Sicily, Italy, showing the oldest diatremes along the Anapo River (blue), the Cozzo Ferrante diatreme (green) and the Costa Giardini diatreme (pink) to the north. The red square indicates the area magnified in B. (b) Geologic sketch map of the Costa Giardini maar-diatreme area, east of Sortino. Lithostratigraphic unit as described in the text. The blue lines NW-SE and N-S indicate approximate location of sections shown in Fig. 5



alternative mechanism that phreatomagmatic activity was responsible for maar-diatreme emplacement in a submarine environment.

### Geological survey

To the east and south-east of Sortino, where Carbone and Lentini (1981) first mapped diatreme facies, we have recognised at least 5 individual diatremes (Fig. 2a), here described from south to north and from the lowest to highest stratigraphic position. Three of these diatremes are exposed along the Anapo River in outcrops at the lowest stratigraphic position, between ~170 and 220 ma.s.l. These are deeply eroded and very likely coeval because they are exposed at roughly the same stratigraphic level with nearly horizontal bedding. These exposures are separated stratigraphically by several tens of metres of limestone from the majority of the exposures of the Cozzo Ferrante diatreme to the north (Fig. 2a). This feature has a diameter of about 500 m, is exposed between about 200 and 300 ma.s.l., forms almost vertical contacts with the surrounding limestones, and is separated laterally by limestone country rock from the Costa Giardini diatreme (CGD), located approximately 100 metres to the north (Fig. 2a). The CGD, at the highest stratigraphic position of all of the potential diatremes, presents many outcrops and an almost complete vertical sequence comprising both the outer tuff ring, eroded or lacking in the others diatremes, and the volcanoclastic sequence filling in the diatreme. Because we consider the Cozzo Ferrante and Anapo diatremes as older than the CGD, we focus here only on the CGD pipe conduit and its associated volcanic products (Fig. 2b).

The outcrops of the CGD are exposed about 2 km east of the Sortino village in an amphitheatre-shaped depression ~1.8 km wide and 285 m deep (Fig. 2a, b) that almost perfectly preserves the original morphology of a broad crater excavated within the limestone sequence. The CGD, which has been deeply dissected by erosion, was emplaced within the sequence of CF as defined by Grasso et al. (1982, 1983). Roads that wind down from the northern margin of the depression, at ~500 ma.s.l., to the Anapo River valley to the south provide almost continuous outcrop exposure of the vertical sequence of maar-diatreme lithostratigraphic units. The upper part of the complex, the crater, has a saucer shape cut into the basal limestone sequence (Figs. 3 and 4), with gentle slopes down to ~400 ma.s.l. Given that the bottom of the crater is located below the surrounding topographic surface and has gentle dips (Fig. 3), we consider this structure a maar (Lorenz 1986; Cas and Wright 1988; White 1991; Németh et al. 2008). The slopes steepen below 400 ma.s.l. until ~300 ma.s.l., below which the depression flattens towards the exposed base at ~215 ma.s.l. (Fig. 2b).

Within and surrounding the CGD we identified seven distinct lithostratigraphic units. The descriptions of these units follow the non-genetic terminology suggested by White and Houghton (2006) and Cas et al. (2008a, b), and are followed by our interpretation of the observed features. These features are also summarised in Table 1. Thus we apply the following terms: *breccia* to any lithified sedimentary deposit with angular grains coarser than 2 mm (White and Houghton 2006); *lapilli tuff* to any lithified primary volcanoclastic deposit having grain size between 2 and 64 mm (with fine, medium and coarse lapilli tuff being in the range between 2–4 mm, 4–16 mm, and 16–64 mm,

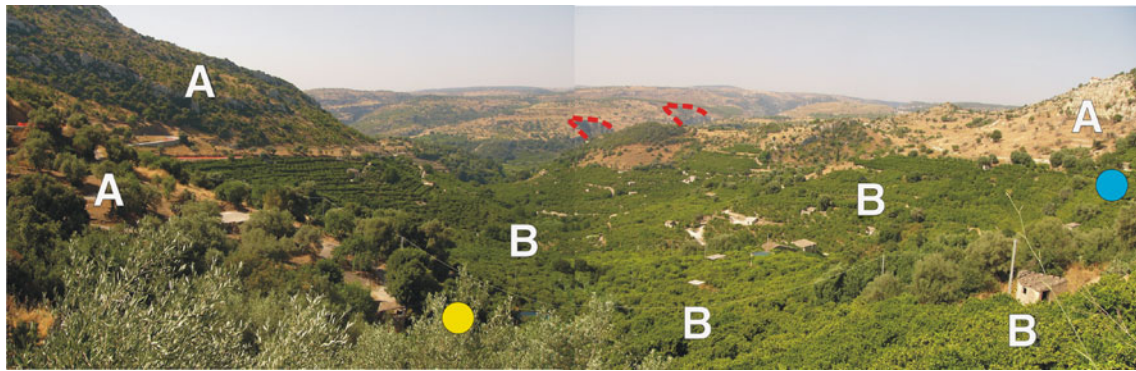


**Fig. 3** Photo of the Costa Giardini diatreme taken from NE, showing the limestone country rock (a) to the east (left margin of the photo) and to the west (right margin of the photo). Trees are grown on the diatreme breccia (b). Two older diatremes that we have recognised along the Anapo River are shown in the background outlined by

dotted red lines (compare with Fig. 2a). These were included by Carbone and Lentini (1981) within the CGD sequence. The yellow circle shows the outcrop of Unit 4 (hyaloclastite), and the blue circle the outcrops of Unit 5 (dikes and plugs)

respectively; White and Houghton 2006); and *volcaniclastic* to any aggregate that consists of volcanic fragments, irrespective of the mode of fragmentation or final deposition (Cas et al. 2008b). The lithostratigraphic units we recognize are as follows: Unit 1 - the limestone country rock that underlies and surrounds the CGD; Unit 2 - a ring comprising bedded and stratified lapilli tuff that occurs at the top and surrounding the CGD; Unit 3 - crudely bedded to nonbedded volcanoclastic breccia, with extremely variable clast size and composition (volcanic and limestone) that occurs at all depths within the CGD interior; Unit 4 - finely laminated, medium lapilli tuff breccia that occurs within the CGD; Unit 5 - massive magmatic intrusions at several locations within and at the margins of the CGD; Unit 6 - interbedded laminated limestone and subordinate thin layers of friable volcanoclastic sediments near the top of the CGD sequence; Unit 7 - upper marine limestones overlying Unit 2 and Unit 6. The mutual contacts between these lithostratigraphic units are shown in two sections

(Fig. 5). The units that we describe below are dissected by a number of normal faults, mostly vertical or nearly so. Some of these intersect the CGD at high angles, but others trend at low angles to the sides of the CGD (Fig. 2b). Notably, some of these faults assume a roughly concentric pattern surrounding the CGD (Fig. 2b), which is quite different from the NE-SW general structural trend of the area (Grasso et al. 1982, 1983).

### Description and interpretation of lithostratigraphic units

#### Unit 1 description

*Country rock* White, fine to coarse-grained bioclastic packstone to grainstone limestones underlie and surround the volcanic and volcanoclastic rocks of the CGD, and comprise Unit 1. Grasso et al. (1982), mapped the area

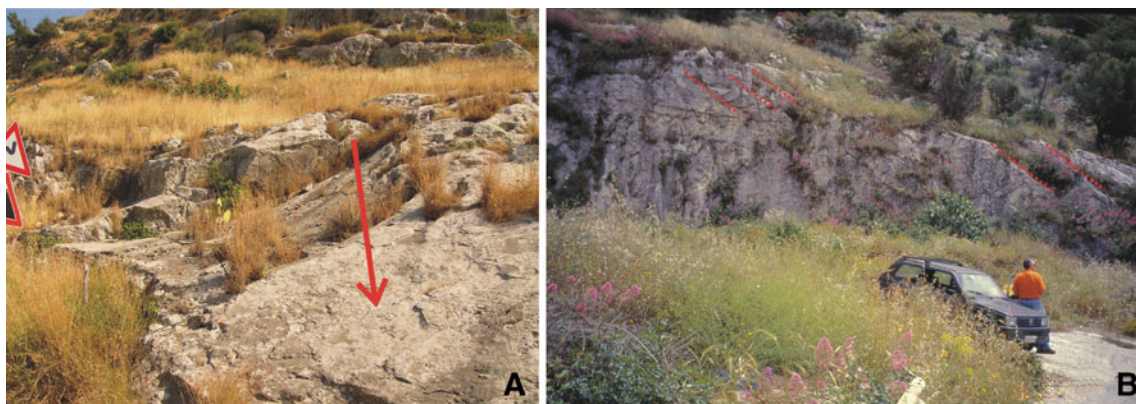


**Fig. 4** Outcrops of Unit 1 country rock bounding the north upper part of the CGD along the main road at about 360 m.a.s.l. **a:** saucer-shaped country rock showing polished surfaces (orange arrow pointing at it).

**b:** View of the quarry wall showing a section of the Unit 1 country rock with joints parallel to the upper surface sloping towards the diatreme centre, evidenced by dotted orange lines

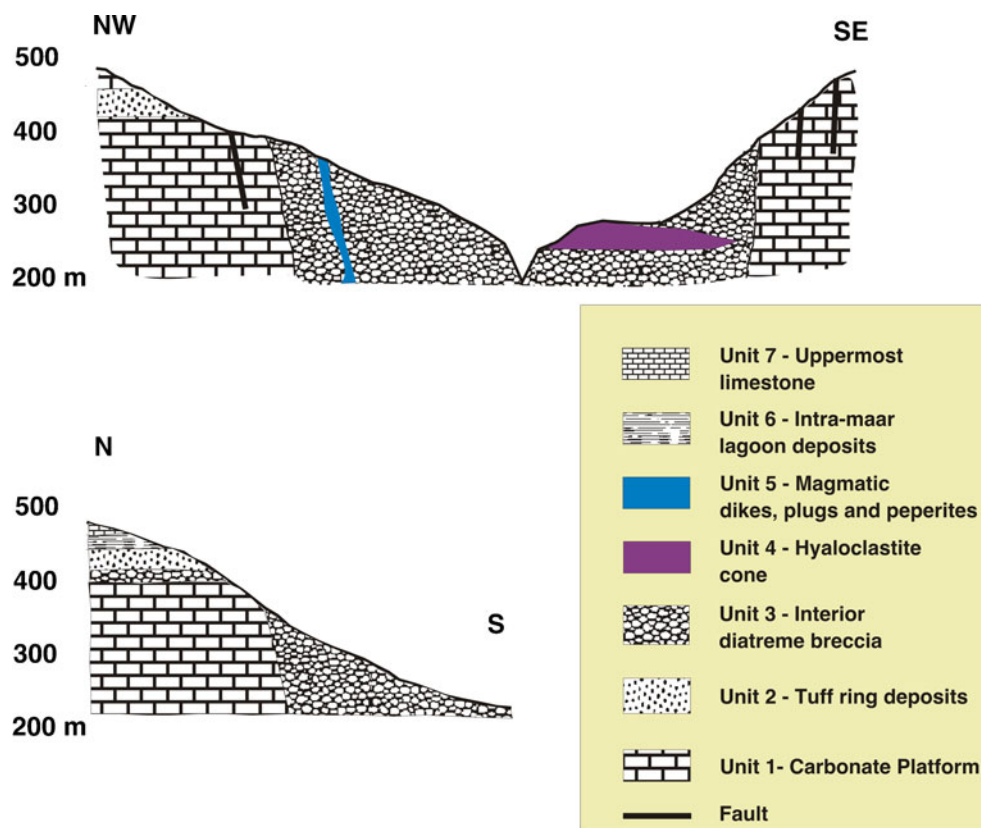
**Table 1** Main features of the Costa Giardini Diatreme (CGD) lithostratigraphic units

	Description	Prominent features	Interpretation
Unit 1	Country rock	Bedded wackestone to grainstone	Carbonate platform deposits
Unit 2	Bedded lapilli tuff	Well to crudely stratified, lava and limestone clasts, ultramafic xenoliths, accretionary lapilli, impact sags, dune forms	Tuff ring
Unit 3	Volcaniclastic breccia	Crudely to non-stratified, lava and limestone clasts, armoured lapilli	Inner diatreme breccia
Unit 4	Laminated lapilli tuff	Finely laminated, hyaloclastite	Subaqueous hyaloclastite grain flow deposits
Unit 5	Mafic bodies	Tabular, chilled margins, locally brecciated, contacts with breccia or country rock	Late-stage intrusions of low-volatile magma
Unit 6	Thinly bedded limestone	Laminated to thinly bedded, soft-sediment deformation features, interbedded volcaniclastics	Intra-maar lagoon
Unit 7	Uppermost limestone	Marly limestone with root traces to grainstone	Paleosol overlain by shallow marine carbonates

surrounding the CGD as the (Tortonian) CF, which in the type area comprises only 45 m of volcaniclastic rocks and interbedded biohermal limestones. Grasso et al. (1982) and Schmincke et al. (2004) ascribed volcaniclastic rocks of the CGD to the CF, but describe the surrounding limestone country rock as the Siracusa Limestone Member of the Monte Climiti Formation, which underlies the CF. We follow this usage for the limestone country rock that forms the walls of the CGD, where it outcrops on the rim of the CGD, and where it is exposed by erosion of the intervening volcaniclastic breccias.

Unit 1 is well exposed within the CGD between 360 and 350 ma.s.l. along the road that descends into the structure. Along the north wall of the diatreme, the limestone outcrops display polished surfaces (Fig. 4a) that dip towards the centre of the CGD (south to southwest). Commonly, these surfaces are listric, with the dip of the surface decreasing in the downslope direction from 40° to <10°, imparting a pronounced saucer-shape morphology to the middle part of the CGD. A small limestone quarry along the E-W road at ~330 m (Fig. 4b) exposes sub-horizontal fractures parallel to the outer surface of the polished limestone, with dips that also

**Fig. 5** NW-SE and N-S stratigraphic sections through the CGD, showing the vertical and lateral unit relationships. See Fig. 2b for locations of sections



are oriented towards the centre of the diatreme, but no slickensides were observed on these polished surfaces.

#### Unit 1 interpretation

*Carbonate platform* We consider the limestone sequence described above as comprising the carbonate platform of Grasso et al. (1982, 1983) within which the CGD was emplaced. The polished surfaces are detachment surfaces along which limestone blocks slid as they slipped into a void created by the explosive removal of the country rock within the CGD. The lack of slickensides might be due to low confining pressure as the explosion and fragmentation that created the crater occurred at a shallow subsurface depth; blocks slumped into the opening created by explosive dislodgement of country rock without significant vertical loading. The joints that are parallel to these surfaces, or nearly so, may be either partially aborted detachment surfaces caused by the proximity to the explosion centre, or alternatively, exfoliation joints resulting from the release of confining pressure (Fig. 4b). Along the west and east walls of the CGD, the face of the limestone outcrop is exposed only sporadically where the outcrop face dips steeply; the gentle slopes of the upper to middle part of the CGD are covered by colluvium. High-angle fault contacts between the limestone and the Unit 3 volcanoclastic breccias are common along the west and east walls of the CGD (Fig. 2b).

#### Unit 2 description

*Bedded lapilli tuff deposits* The rim of the CGD is surrounded by the eroded remnants of bedded and stratified lapilli tuff of Unit 2 (Fig. 6a-d). These beds outcrop at several locations to the north, northwest and east of CGD, between 460 m and 490 m (Fig. 2b). Elsewhere, the unit is missing, presumably due to erosion possibly enhanced by fault displacement.

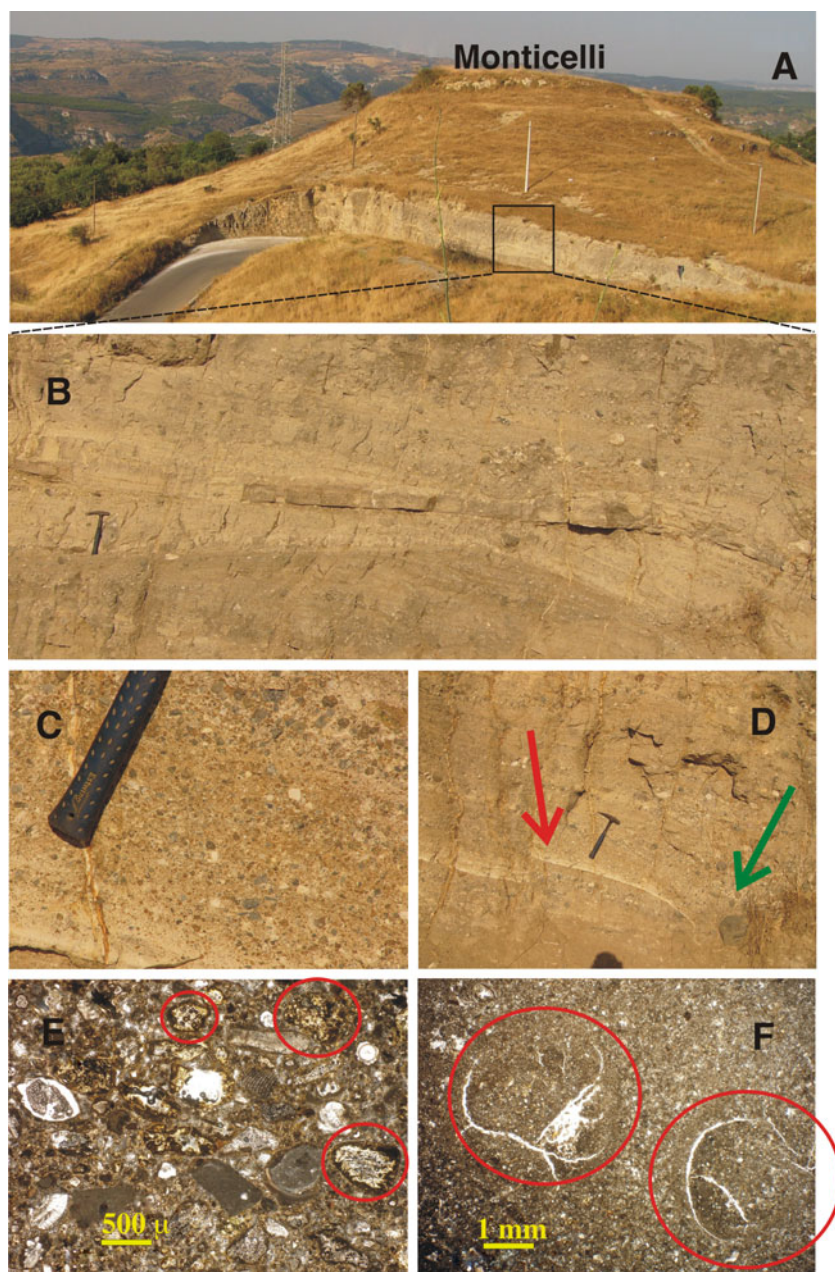
The most extensive exposure is along the road that descends into the CGD at Monticelli, where it attains the maximum thickness of ~30 m. Here, this unit consists of volcanoclastic beds, 10 cm to 50 cm in thickness, with generally very distinct bed boundaries marked by abrupt changes in grain size (Fig. 6d). Bed fabric varies from nongraded to normally graded to inversely graded (Fig. 6c), with some beds displaying distinct internal cross-stratification (Fig. 6b). Clast size in most beds varies from sub-centimeter to >10 cm, but outsize clasts (>20 cm) also occur (Fig. 6d), either isolated within beds of much smaller clasts or, more often, concentrated with other outsize clasts within a lenticular bed or at the top of an inversely graded

bed to form impact sags. Impact sags contain angular blocks of both limestone and nonvesicular massive lava. Coarser-grained beds typically display a clast-supported fabric. The matrix of the beds is dominantly a mixture of fine-grained carbonate grains, including a high contribution of bioclasts, and micritic calcite, with a smaller contribution of fine-grained, vesicular and generally well-rounded clasts of sideromelane, typically with palagonite rims (Fig. 6e).

Clasts vary from angular to well rounded, and comprise both mafic lavas and limestones. The lava clasts are angular to well-rounded, poorly vesicular to nonvesicular, commonly glassy or weakly porphyritic (Porphyritic Index PI up to 10%), with maximum size of 18 cm but generally of ~3 cm in size, and with variable alteration. Limestone clasts are up to 30 cm in diameter but generally 1-3 cm in size and are white to pale yellow. The lithology of the limestone clasts varies from micritic to grainstone, and sometimes consists of individual bioclasts (e.g. corals). A few limestone pebbles exhibit an outer rim that is slightly orange colored that contrasts with the lighter interior. The rims and interiors of several limestone clasts were analyzed isotopically to test for thermal alteration of the carbonate, but the analysis revealed no significant difference in isotopic composition. In some instances, beds thinner than 10 cm are separated by distinct cm-scale fine-grained layers (Fig. 6c). These thin individual layers often contain abundant accretionary lapilli (Fig. 6f). The accretionary lapilli (*sensu* Gilbert and Lane 1994; Schumacher and Schmincke 1995) are up to 0.5 cm in diameter, and may be formed by a minute core of volcanic ash (much less than 10% of the total size), or the core may consist of fine-grained carbonate, surrounded by multiple layers of very fine-grained carbonate particles (Fig. 6f).

Within the 30-m section on the road below Monticelli, the beds in the lower 10 m of the section generally contain larger clasts and are more commonly nongraded, and lack internal stratification. The upper 20 m of the section, in contrast, is characterized by more distinct bedding features caused by the abrupt changes in grain size. Bedforms in this section include truncation surfaces, scour and fill structures and convex (dune) forms with internal cross-lamination with dip directions oriented away from the center of the CGD (Fig. 6b). Other features of this part of the section include the presence of (rare) ballistic impact structures (Fig. 6d) and common accretionary lapilli (Fig. 6f). The uppermost 8 m of section exposed on the hillside north of Monticelli reveals alternating fine and coarse-grained beds, 2-10 cm thick, nongraded to weakly inversely graded beds with scour and fill structures with up to 0.5 m relief. Lava blocks in the beds are up to 60 cm, and xenoliths of pyroxenite up to 7 cm are abundant, and sometimes coated by basalt. The section is capped at the top of the hill by a fine-grained, orange, gastropod-bearing limestone, which is overlain by shallow marine bioclastic limestone, described below (Unit 7).

**Fig. 6** Features of Unit 2. **a:** View from top of the Monticelli Hill, with Unit 2 cut by the road. At the very top of the hill Unit 7 is exposed. The black square indicates the area blown up in B. **b:** close-up view of the sand-wave beds from Unit 2 illustrating the cross-stratification; hammer for scale. **c:** close-up view of the inverse grading of breccia beds in Unit 2. **d:** Fine-grained bed (just below the hammer) that is offset by a fault to the left (evidenced by red arrow). Ballistic impact with a large lava block visible to the lower right (evidenced by green arrow). **e:** thin section micrograph of Unit 2 matrix consisting of carbonate bioclasts (grey) and vesicular sideromelane grains (brown, within red circles), plane polarized view. **f:** thin section photomicrograph of two accretionary lapilli (within red circles) in Unit 2 consisting entirely of micritic carbonate, plane polarized view



### Unit 2 interpretation

*Tuff ring deposits* We interpret the coarse, nongraded to graded lapilli tuff breccias of Unit 2 comprising the lower portion of the sequence as the deposits primarily of high concentration sediment gravity flows, such as subaqueous debris flows. Volcaniclastic density currents in shallow, subaqueous settings have been interpreted as the result of the collapse of jets of ejecta produced by Surtseyan explosions and by slumping of oversteepened accumulations of tephra (White 1996; Martin et al. 2004; Sohn et al. 2008; Brand and Clarke 2009; White and Houghton 2000). Deposits from slumping suggest that the early explosive

activity produced a cone of tephra located closer to the initial eruptive vent than the preserved ring of material exposed in outcrops. Oversteepening through continued accumulation may have caused frequent collapses that produced the high density, nongraded gravity flows. More dilute density currents were generated by slurries formed by the reentry into the water of tephra ejected as Surtseyan jets. The debris-flow process in a subaqueous setting commonly produces beds that display inverse to nongraded bases, and also may produce normally graded bed tops (Nemec and Steel 1984), as seen here. The commonly well-rounded clasts additionally indicate transport in a dense medium where clasts can collide and abrade such as in

turbulent high-concentration density currents or the bases of stratified currents. The presence in these beds of impact sags and ballistic blocks of both limestone and nonvesicular lava is consistent with the interpretation of explosive (hydromagmatic) activity involving volatile-poor magma and strong disruption of the country rock.

The finer-grained lapilli tuffs that display crossbedding, internal truncation surfaces, scours and dune forms (or sandwaves) observed in the upper part of the sequence (Fig. 6b) we interpret as the deposits of traction currents, potentially subaerial base surges (Fisher and Waters 1970; Cas and Wright 1988; Sohn 1995; Aranda-Gómez and Luhr 1996) formed by the collapse of a steam-rich eruption column. The presence of accretionary lapilli, formed by deposition of the finely powdered limestone country rock from either a damp (steamy) subaerial eruption plume or in base surge currents, further suggests conditions of water exclusion, at least within the vent (Gilbert and Lane 1994; Schumacher and Schmincke 1995). The composition of these accretionary lapilli, consisting essentially of multiple rims of fine limestone particles, indicates a high level of fragmentation of the country rock. The finest-grained cm-scale beds that separate some of these beds may have formed by tephra fallout (Kokelaar and Durant 1983; Cas et al. 1989; Sohn 1995; White 1996).

The upward transition from poorly sorted sediment gravity flows to sandwave units in subaerial maars and/or tuff rings has been documented in several studies and attributed to the decreasing availability of water. Lefebvre and Kurszlauskis (2008), for example, noted an upward decrease in bedding thickness that they interpreted as recording the progressive decrease in explosive force from declining water availability. The same authors noted further that the deepening of the explosive centre due to restricted water access could result in explosive sampling of progressively deeper material. This potentially could explain the greater abundance of pyroxenite clasts in the upper tuff ring of the CGD; these may represent magma cumulates or, alternatively, xenoliths from the mantle (Scribano et al. 2009). Nevertheless, the common presence of sideromelane, rather than tachylite, in many of these beds argues for fast cooling, and can be indicative of a wet eruptive environment, as the formation of sideromelane glass indicates rapid quenching of the basaltic magma. This is not contradicted by the presence of the accretionary lapilli, however, as a steam-rich eruptive column forming a water-exclusion zone (Kokelaar 1983) may allow particle accretion as armoured lapilli (White 1996) or accretionary lapilli to form even in a subaqueous environment (Martin et al. 2004). In fact, although lapilli commonly have been used to identify subaerially erupted tephra, recent studies show that their formation is also possible in subaqueous settings within the steam envelope of the eruption column

(Martin et al. 2004). The ballistic sags described, however, indicate plastic deformation of bedding, and are most consistent with an interpretation of a wet/damp subaerial environment, due to both reduced impact energy and the difficulty of making fully subaqueous cohesive deposits.

The deposits of Unit 2 comprise the outer tuff ring, which formed initially on the submerged carbonate platform (Unit 1). The high proportion of fragments from carbonate rock that was lithified before the eruption, in comparison to the volcanic products, in both the framework clasts and the matrix of the breccias, indicates very strong shattering of the country rock and a subordinate contribution of the magmatic component during the early stages of the eruption. The innermost cone-forming portions of the ejecta ring surrounding the maar undoubtedly collapsed back into the crater as the maar widened during the early stages of the eruption and were recycled by continuing explosive eruptions. This is suggested by the lack of outcrops of this unit on the south portion of the diatreme (Fig. 2b), by the presence of meter-sized blocks of enclosing limestone country rock, and by the debris-flow units from the unpreserved cone characterising the lower portion of the ring. In addition, the inward sliding of larger blocks of country rock, indicated by the listric polished surfaces of Unit 1 along the north wall of the diatreme (Fig. 4a), widened the crater, thereby undercutting the proximal portions of the tuff ring. The portions of the tuff ring that slumped into the explosion crater were reworked by mixing with both country rock and fresh magma by continuing explosions and formed the breccias of Unit 3 (see below). The remaining ring has subsequently been eroded and dissected along the north side by a number of normal faults, mostly vertical and trending N-S (Fig. 2b). The preservation of this unit along the north, north-western and eastern parts of the CGD suggests that no major inward collapses affected these portions of the structure after emplacement. Increased magma rise rates is evidenced by the presence of xenoliths (pyroxenite) in the upper part of the tuff ring, these commonly being regarded as indicators of mantle source for these magmas (e.g. Scribano et al. 2009). Deepening of the explosive center below the crater floor is demonstrated by the near vertical contacts between the country rock and Unit 3 (see below).

### Unit 3 description

*Massive volcanoclastic breccia deposits* The majority of the interior of the CGD is filled by the coarse volcanoclastic breccias of Unit 3. Outcrops of this unit occur along the walls of the CGD from as high as 460 ma.s.l. to the lowermost exposures in stream beds at the very base of the CGD, at about 215 ma.s.l. (Fig. 2b). In the upper part of the CGD (above

350 ma.s.l.), there are several locations on the eastern and western walls where this unit occurs in fault contact with the limestone country rock (Unit 1). In general, exposures of this unit are nonbedded to very crudely bedded, most commonly lacking any distinct structure or organization (Fig. 7a-e). One exception occurs in the uppermost part of this unit on the NE

margin of the diatreme (Fig. 2b), where thinly bedded (5 cm to 20 cm thick beds) Unit 3 breccia is in depositional contact with Unit 1 at an attitude of 80° (Fig. 8a-b). In several locations, large blocks (some up to tens of metres long) of the country rock are superposed over the breccia (Fig. 8c). The texture of Unit 3 represents a continuum of particle

**Fig. 7** Features of Unit 3. Photos **a**: Nonbedded breccia consisting almost entirely of limestone clasts. **b**: multiple armoured lapilli (evidenced by *black circles*) consisting of clasts of the breccia matrix surrounded by a carbonate rim (*pencil* points at the top for scale); an amphibole crystal is the black grain below and right of the *pencil* point. **c**: breccia showing distinctive finer-grained light and coarser-grained dark domains oriented vertically. **d**: vesicular lava block within the breccia. **e**: immediately above the *pencil* is a limestone country rock clast; light and dark domains are distinguishable, with different proportions of volcanic clasts. **f**: thin section photomicrograph of nonbedded breccia showing very well rounded volcanic clast at the top; large clast at the bottom of the photo is bioclastic limestone, plane polarized view. **g**: variety of volcanic clasts including abundant tachylite (*black grains*), plane polarized view



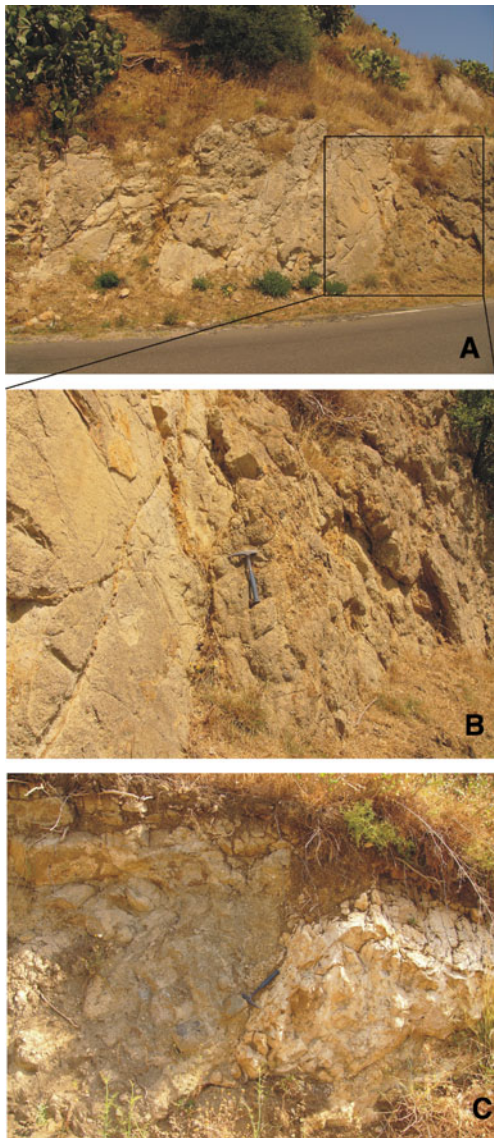


**Fig. 8** Features of Unit 3 breccia. **a:** along the upper road at about 440 m a.s.l., contact between limestone country rock and breccia at high inclination. **b:** magnification of the square in A. **c:** limestone block emplaced above the breccia on the east wall of the diatreme, at an elevation of about 300 m a.s.l

sizes, from granules to boulders of 1 m in diameter or more. Boulders are outsize clasts and usually represent only ~5% of the rock volume. Lava clasts are from subangular to subrounded, from poorly vesicular to nonvesicular, in places oxidized, finely crystalline and with PI between 10 and 30%; their relative proportion generally varies from ~20% to ~80% of the rock volume, although in a few isolated instances, the breccia appears to consist almost entirely of limestone (Fig. 7a). Large limestone clasts are up to 1 m, but most limestone clasts are 0.5 to 1 cm wide. Limestone clasts include large blocks of wackestone, packstone and grainstone as well as individual bioclasts (coral). The texture of many limestone pebbles indicates that they are recrystallized.

The proportions of lava and limestone clasts in the breccias is extremely variable, as it is in the matrix. Accretionary lapilli do not occur in this unit, although armoured lapilli, several millimeters to several centimetres in diameter, are locally abundant, especially along outcrops located at about 300 m elevation in the middle portion of the exposed inner diatreme (Fig. 7b). Armoured lapilli in this unit usually comprise a wide core (more than 50% of the total size) consisting of breccia matrix and one or more thin outer rings consisting of carbonate particles. The breccia matrix comprises variable proportions of sand-sized grains of volcanic particles, including both abundant tachylite and sideromelane, limestone and occasional free (unincorporated) crystals of pyroxene, up to several centimetres long, all surrounded by a finer grained mixture of micritic calcite and palagonite (Fig. 7f-g).

In some locations, the breccia displays pronounced domains, defined by variations in texture or colour due to abrupt variation in clast or matrix composition (Fig. 7c). These domains are discontinuous regions, and so do not constitute bedding; they may, however, be related to processes of deposition. In other places the breccias exhibit parting surfaces that appear to follow subtle changes in grain size, and so may represent crude bedding. The orientation of these features suggests that most of the breccias in the middle to upper part of the CGD were emplaced at very high angles, dipping into the CGD interior, as described above. Generally, however, these features do not display the abrupt differences in grain size and texture that are associated with direct deposition from “debris jets” (McClintock and White 2006; Ross and White 2006; Ross et al. 2008).

### Unit 3 interpretation

*Interior diatreme breccia* The coarseness of these breccias, together with the general lack of organization, suggests that Unit 3 breccias were emplaced by different processes than those responsible for the well-stratified deposits of Unit 2. Whereas Unit 2 breccias were formed by deposition through mass flow and traction currents (debris flow and surge) of material ejected from the volcanic vent at the CGD, the breccias of Unit 3 apparently represent the accumulation of material that fell back into the volcanic crater, either through simple ejection and fall-out, or through sloughing of material that had accumulated around the rim. Indeed, the steep angles of repose of these deposits, where bedding is visible, indicates slumping and/or avalanching of breccias from higher elevations. Contacts where country rock is superposed over the breccia resulted from spalling of the country rock from the walls of the crater as it widened, potentially both during and after the

explosive activity. Both country rock and breccia that slid into the crater during ongoing explosive activity had the potential for mixing and reworking within the crater. Lorenz and Kurszlaukis (2007) noted the occurrence of “well-mixed tephra” in the upper root zone of diatremes. We interpret the abrupt variations in texture and colour domains within some breccia outcrops as the result of this reworking process, whereby portions of breccia with differing characteristics were mixed within crater. The distinct textural domains in the breccia suggest that the recycling of the volcanoclastic breccia occurred by fragmentation of previously deposited breccia that was already partially consolidated (Gilbert and Lane 1994; Schumacher and Schmincke 1995). The abundance of armoured lapilli in these breccias would seem to indicate that the mixing took place in a steam-rich volcanic plume. The occurrence of tachylite, which is not present in the Unit 2 lapilli tuffs, further suggests a reduced role for water in the vent, as tachylite forms by the more gradual cooling of the basaltic magma (Fisher and Schmincke 1984; Martin et al. 2004). Additional evidence of the presence of a drier vent is the crystallinity of magmatic clasts, that also lack a glassy rim that would have formed in case of contact with water.

One notable breccia outcrop occurs at the far western margin of the diatreme, possibly beyond the actual wall of the diatreme pipe (Fig. 2b). This breccia (surrounding the intrusions in Fig. 9) consists entirely of fragmented country rock, suggesting that it is a “contact breccia” (Lorenz and Kurszlaukis 2007), which may form in overhangs or zones laterally equivalent to the diatreme through shock and rarefaction.

#### Unit 4 description

*Finely laminated medium lapilli tuff breccia deposits* An outcrop of finely laminated medium lapilli tuff breccia that occurs at low elevation (260 m a.s.l.) on the eastern side of

the CGD (Fig. 2) constitutes Unit 4. The outcrop has a stratigraphic thickness of ~20 m and dips to the east-northeast (70° to 85°) at angles of 65° to 20°, decreasing to the east. In the lower part of the sequence, the rock framework consists typically of ~90% lava clasts and ~10% limestone clasts (Fig. 10a). The lava clasts are dark black with a glassy appearance, are mostly nonvesicular to poorly vesicular, are subangular to subround, and are mainly 0.2 to 1 cm in diameter, with rare oversize clasts up to 6 cm. The limestone clasts are white and 0.5 to 1.0 cm in diameter. The beds are well-stratified, with bed thickness between 0.5 to 5 cm distinguished by alternating fine and coarse layering (Fig. 10b). The beds display a grain-supported, open fabric filled by calcite cement and show weak inverse to normal grading and local pinching and swelling, but no evidence of basal scouring. Stratigraphically higher in the section, the lithology grades to a limestone-dominated (90%) clast component, with a consequent change in rock colour (Fig. 10c). The upper part of the outcrop consists of cm-scale, evenly bedded conglomerate of millimetre-scale limestone grains (grainstone), with intervening sub-centimetre to centimetre-scale laminae in which volcanic clasts are concentrated. This unit is truncated at the eastern end of the outcrop at 280 m elevation by contact with a block of Unit 3 volcanoclastic breccia.

#### Unit 4 interpretation

*Bedded hyaloclastite cone* The glassy, fine-grained nature of the volcanic clasts in these beds suggests that they are hyaloclastites that originated by nonexplosive, subaqueous fragmentation of lava in direct or indirect thermal response to chilling by water (e.g. Cucuzza Silvestri 1963; Smith and Batiza 1989; Bergh and Sigvaldason 1991; White and Houghton 2006). The genesis of hyaloclastite, based on evidence in the Iblean area, was deeply discussed by



**Fig. 9** Features of Unit 4. **a:** finely laminated hyaloclastite breccia consisting of ~80% volcanic clasts, western margin of the outcrop. **b:** transition between hyaloclastite-dominated breccia and limestone-

dominated hyaloclastite breccia with a greater amount of limestone clasts in the beds. **c:** finely laminated breccia consisting mostly of limestone clasts with thinner laminae of hyaloclastite



**Fig. 10** Features of Unit 5. **a:** dike at the western margin of the diatreme at about 390 m emplaced at the contact between the country rock (to the *left*) and breccia (*out of view*). The country rock has joints parallel to the orientation of the dike, and the dike displays columnar jointing. **b:** contact surface between dike and breccia at the NW part of the diatreme at about 300 m; the dike has chilled margin and the breccia has thin hornfels zone. **c:** granulation of the dike (below the *hammer*) at the contact with soft limestone-dominated breccia

Rittmann (1973), who proposed that the cooling-contraction granulation of the skin of pillow lavas produces glassy clasts transported, reworked and accumulated by sea currents. If the eruption in a shallow marine environment continues, this process can proceed over time accumulating very thick (up to 200 m) hyaloclastite deposits. We believe that the originally loose hyaloclastites of Unit 4 were soon resedimented, likely by grain flows. In fact, this is suggested by the steep dips, nearly even layering, bed-by-bed variations in grain size and inverse to normal grading (e.g. Tanner and Calvari 1999). In addition, these grain flows incorporated

bits of the limestone country rock previously granulated, with an increasing proportion of accidental lithic versus juvenile components going upwards in the sequence. The consistent slope direction of the deposit towards the eastern wall of the CGD, rather than towards the interior, suggests that these grain flow deposits accumulated on the flank of a structure, perhaps a submerged cone, that grew within the CGD crater at a time when the depression was water-filled and the extrusion rate was extremely low (Wohletz 1986). Alternatively, we note that the elevation of this deposit is more than 200 m below the rim of the CGD, thus the water depth (and hydrostatic pressure) may have been sufficient to prevent explosive interactions between rising magma and water (Lorenz 1986), given that the fragments are nonvesicular and thus the magma was reasonably volatile poor (cf. Schipper et al. 2010).

#### Unit 5 description

*Non-fragmental, intrusive magmatic bodies* This unit consists of small magmatic bodies with a basaltic composition that occur at the margins of the CGD. Several of these are exposed between 300 and 350 m elevation along the western margin of the CGD (Fig. 2). Most commonly these occur at the contact between the country rock (Unit 1) and the Unit 3 breccia (Fig. 9a), although some are observed intruding directly within outcrops of the Unit 3 breccia (Fig. 9b). Often, the intruded unit, either country rock or breccia, displays jointing parallel to the orientation of the intrusive body (Fig. 9a). The outcrop exposures are a few meters wide and up to a few tens of meters high, and elongate in a nearly N-S orientation (e.g. 160°). Commonly, these outcrops display chilled margins and columnar jointing (Fig. 9a). The basalt consists of <5% plagioclase microphenocrysts, ~1-3 mm long, within a black glassy groundmass. It is poorly to nonvesicular, with mm-sized vesicles (where present) concentrated in the outer shell.

In some instances, the contact between the intrusion and the breccia is marked by a thin (5 cm wide) hornfels zone. In one location on the far western margin of the CGD, the contact between the intrusion and the Unit 3 breccia is an irregular surface with abundant basalt blocks floating within the breccia near the intrusion (Fig. 9c).

#### Unit 5 interpretation

*Magmatic dikes, plugs and peperites* The shape and contact relationships of the magmatic intrusions described above lead us to interpret them as late stage dikes and plugs, with subordinate granulation of the magmatic intrusions at the contact with incompletely lithified country rock. This granulation appears to be evidence that the intrusion was

emplaced while the breccia was not yet consolidated, causing it to granulate and break into pieces at the contact (cf. McClintock and White 2006). The interaction between magma and wet, unconsolidated sediments is known to cause in-situ disintegration of the magma, forming the rock called peperite (White et al. 2000; Skilling et al. 2002; Németh and White 2009). The blocky, subequant to tabular clast morphology we see in association with the intrusion shown in Fig. 10c is consistent with this mode of formation. However, the general association of intact magmatic intrusions with the breccias indicates a lack of explosive activity related to late stage magma rise, although the presence of glassy outer surfaces in the magmatic intrusions suggest rapid cooling, and that the volcanoclastic breccia was wet at the time of the intrusions. The fact that the late stage dikes and plugs are poorly to nonvesicular shows that the basalt is volatile-poor. Locally, as at the location of the dike in Fig. 10a, the breccia consists entirely of fragmented country rock, the “contact breccia” of Lorenz and Kurszlauskis (2007), which may form in overhangs or zones laterally equivalent to the diatrema through shock and rarefaction.

#### Unit 6 description

**Thinly bedded limestone** This unit is exposed at a single location on the northeastern rim of the CGD between 460 m and 475 m a.s.l. (Fig. 2b). The 15 m-thick section, which has a lateral extent of about 200 m, consists of finely laminated to thickly bedded limestone interbedded with layers of poorly lithified volcanoclastic sediments of varying thickness (Fig. 11a). Typically, the limestone has a white to pale yellowish-brown colour, and occurs with varying aspects, including both a mm-scale laminated unit and a thicker-bedded unit consisting of centimetre-scale to decimetre-scale beds. The fine laminae of the laminated unit stand out in outcrop due to weathering, which accentuates the compositional alternation between micritic and sparry calcite laminae. The texture of the laminated unit varies from nearly evenly, parallel laminae to wavy or crinkly, and locally to a brecciated texture, comprising discontinuous, broken laminae

**Fig. 11** Features of Unit 6. **a:** north wall of the diatrema showing thinly bedded to thinly laminated limestone with dm-scale bed of volcanoclastic sediment at the top (brown); outcrop section is about 2 m thick, exposed along the upper road at about 460 m a.s.l. **b:** limestone illustrating bedding disruption by rapid dewatering, cropping out at ~460 m a.s.l.

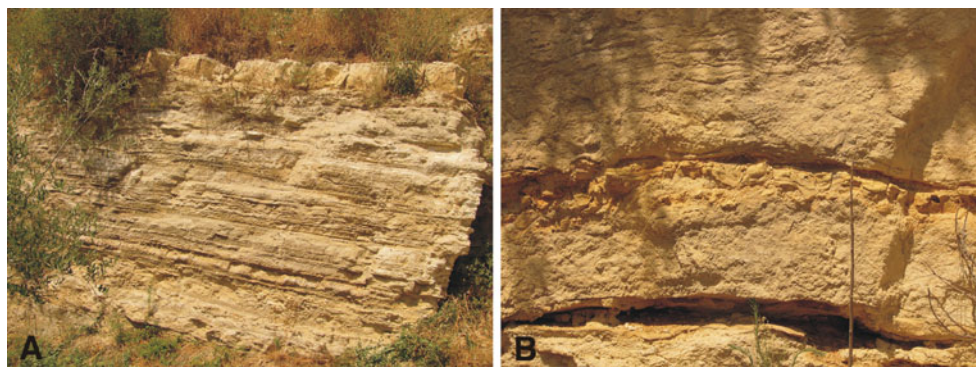


(Fig. 11a-b). Some centimetre-scale beds appear to consist entirely of completely disrupted laminae. Thicker bedded limestones may also be laminated, but the laminae are not prominent on the outcrop face, or they may show evidence of bioturbation, or they may be structureless.

Interbedded with the limestones are thick-bedded layers of marl comprising a mixture of varying proportions of coarse volcanoclastic grains and carbonate. Individual beds vary in thickness from a few centimetres to 0.5 m, and are typically nongraded. These beds generally weather to light yellowish-brown colour and vary from fine to coarse grained, with volcanic clasts up to 2 cm in diameter. The contacts between beds show substantial variations, with some exhibiting even, conformable contacts and others displaying convex tops, and/or basal loading into the underlying bed. Internal structure of these beds varies from structureless, to convolute laminated, commonly with dewatering structures (Fig. 11b). The section is overlain by limestones of Unit 7 at an elevation of about 475 m a.s.l.

#### Unit 6 interpretation

**Intra-maar lagoon deposits** The laminated limestones of this unit clearly represent accumulation of marine carbonate in a quiet water environment, with the alternation between micritic and sparry carbonate caused by differences in the rate of carbonate production, possibly due to seasonal fluctuations in salinity or sunlight. The process of maar lake formation after the end of diatrema eruptions is very well described, and commonly a result of the groundwater table restoring itself to the original levels after the eruption ends (e.g. Kienle et al. 1980; Lorenz 1986; Martin and Németh 2005; Németh and White 2009). Here we suggest that, following the cessation of explosive activity, the crater was filled with infiltrating seawater, to a tidal or sea level-controlled elevation, which resulted in formation of an isolated lagoon within the maar ring. Erosion of the enclosing ring provided volcanoclastic material that washed into this lagoon, sometimes through sudden mass-flow processes. This resulted in sudden loading of the sediment

surface with masses of water-laden sediment that produced both dewatering structures and caused disruption of the previously deposited sediments. More gradual erosional processes contributed volcanoclastic sediment that mixed with carbonate to produce the marly sediments within the limestone sequence.

#### Unit 7 description

*Upper limestone* Immediately to the north of the outcrop of Unit 6, the transition between this unit and the uppermost beds of Unit 7 is partially exposed. The limestone immediately overlying the uppermost volcanoclastic bed is a white, marly limestone that is 0.7 m thick and structureless. This is overlain by normal marine bioclastic grainstone. A more complete exposure of this transition occurs on the hill north of Monticelli (Fig. 2b). Here, the top of the exposure of Unit 2 (stratified breccias) occurs at about 490 ma.s.l. Above several metres of covered section, the next exposure consists of 45 cm of fine-grained marly limestone with an orange hue, and containing gastropods and possible root structures, marked by concentrations of Fe-oxides. Overlying this unit are several metres of fine-grained marly limestone to bioclastic grainstone, locally containing large fossils of bivalves. Interbedded with the limestone are several lenticular beds of breccia containing both volcanic blocks, up to 18 cm long, and fossil fragments. These beds are nongraded to inversely graded. The limestone grades to normal marine bioclastic limestone at the top of the hill at 501 ma.s.l.

#### Unit 7 interpretation

*Post-eruptive, shallow-marine limestone deposits* The outcrop of Unit 7 above the laminated, volcanoclastic limestones of Unit 6 demonstrates that the restricted, low energy conditions of sedimentation in the lagoon were succeeded eventually by a return to shallow marine conditions with higher current energies and a normal open marine biota. The outcrop on the hill north of Monticelli presents a more complex record of this transition, however, with quiet, shallow water conditions following the cessation of continuous deposition of the volcanoclastic breccias. The orange unit with possible root traces is a potential paleosol, suggesting an episode of subaerial exposure of the tephra ring. Continued limestone deposition at this location was punctuated by episodic debris flows, although the presence of both bioclasts and volcanic debris in these beds indicates reworking of the volcanoclastic material under increasingly normal marine conditions, which were fully in place by the time of deposition of the uppermost limestone.

## Discussion

### Model for CGD evolution

On the basis of the lithostratigraphic units recognised and described above, we present the following model for the evolution of the CGD.

- 1) During Late Miocene (Tortonian), the area of the Iblean Mountains was a carbonate platform with grainstone and oolite shoals and bioherms (Grasso et al. 1982). These features suggest that water depth across the platform was quite shallow, probably 10 m depth or less given the very shallow depths typical for oolite shoals (2–3 metres; Newell et al. 1960; Hine 1977). Nowhere do we see the actual contact between the tuff-ring deposits that surrounded the maar and the underlying, contemporaneous carbonate platform surface, but as there is no regional evidence for an unconformity at the time of formation of the CGD, we presume that it was on this submerged platform (our Unit 1) that initial explosive activity took place.
- 2) Magma rising along faults in the regional structural regime likely triggered fracturing of the consolidated limestone bedrock at shallow depth and allowed contact between the magma and seawater, resulting in explosive fragmentation of the magma at shallow depth (Fig. 12a). That the explosive force was derived from hydrovolcanic interaction and not the rapid expansion of magmatic gases seems clear from various lines of evidence: the low vesicularity of most of the lava, as indicated in bombs occupying the impact sags (in Unit 2; Fig. 6d) as well as the late stage dikes and plugs (Unit 5; Fig. 9) indicates involvement of a low-volatile magma; the high proportion of carbonate rock fragments in the breccias of the tuff ring dictates that these explosions were fragmenting mostly country rock, not magma, and thus, were likely at a very shallow depth; the permeable nature of the sedimentary environment through which the magma rose would prevent significant overpressure buildup (Lefebvre and Kurszlaukis 2008). This permeability is produced by the presence of faults, joints and fractures at the contact between country rock and diatreme breccia. The shallow depth of the initial explosion site is also indicated by the saucer-shaped surface of the country rock in the uppermost and northernmost exposures of the diatreme structure at about 400 ma.s.l. (Figs. 2b, 4a, b, and 5a, b).
- 3) The initial hydromagmatic explosions excavated a broad, shallow crater into the limestone bedrock (Fig. 12b), with the excavated, pulverized rock, mixed with a minor magmatic component, deposited initially as subaqueous debris flows within the crater (the lower

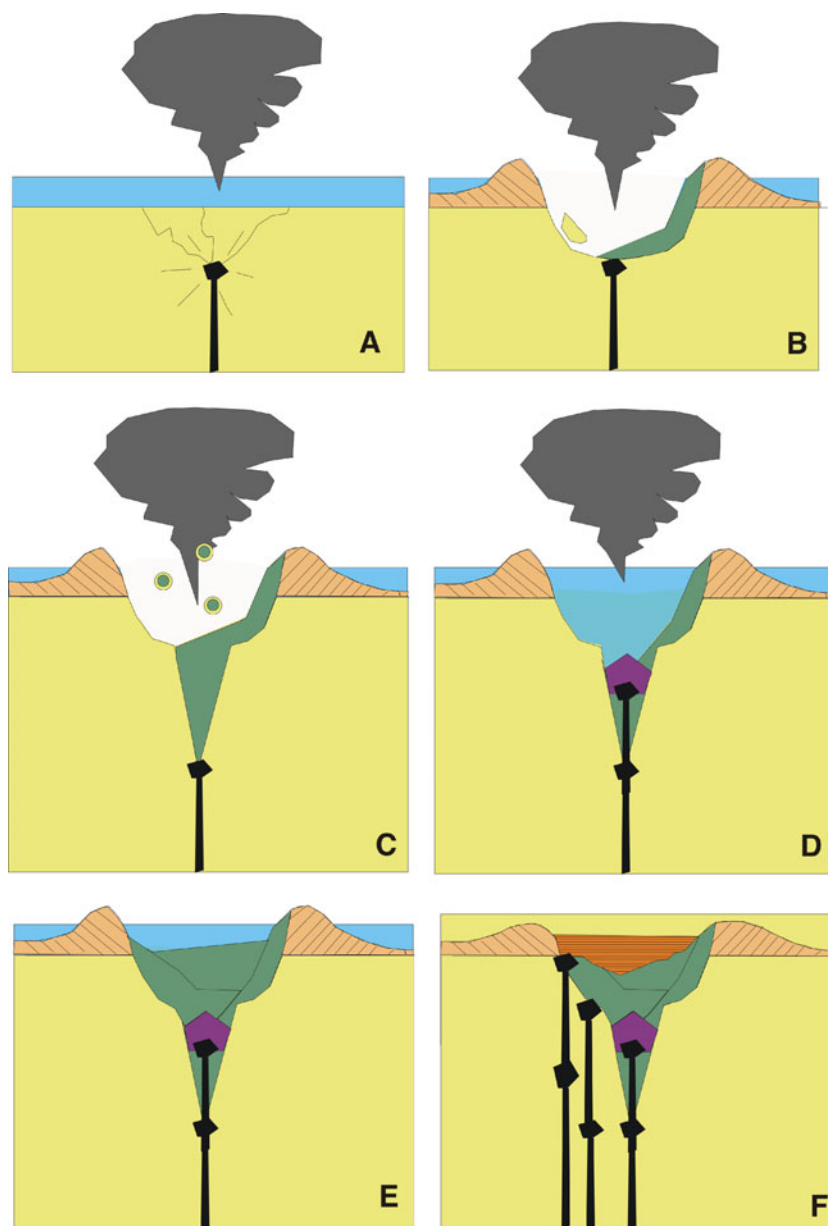


**Fig. 12** Emplacement model for the Costa Giardini diatreme near Sortino. **a:** Early stage of magma intrusion (black) within the submerged carbonate platform (yellow, Unit 1) triggering hydro-magmatic explosive activity. **b:** Shallow explosions excavate the crater, producing bedded lapilli tuff of Unit 2 (tuff ring deposits, light brown) outside the crater and Unit 3 (massive volcanoclastic breccia, green) within the crater, with limestone blocks from Unit 1 falling into the crater. **c:** Deepening of the explosion vent causes the diatreme to grow to increasingly greater depths, without affecting the outer maar, apart from breccia accumulating inside the crater. The ejecta built up around the crater isolates the vent zone from the sea, allowing phreatomagmatic explosions and formation of armoured lapilli preserved in the breccia. **d:** Effusion rate decreases, allowing

infiltration and accumulation of sea water in the crater. Interaction between low-effusion rate lava and water forms finely laminated hyaloclastite breccia comprising Unit 4 (purple). This forms a cone within the crater at a higher level, and is covered by landslides forming the breccia of Unit 3 within the crater. **e:** Erosion of the outer tuff ring ejecta increases accumulation of breccia, debris and landslides within the crater. Explosive activity and reworking of previously deposited material fills the diatreme crater. **f:** Erosion of the tuff ring continues, and final-stage dikes and plugs (Unit 5) are emplaced within the wet breccia deposits of Unit 3 and at the margins of the pipe conduit (contact between Unit 1 and Unit 3). On top of it are very well stratified lagoon sediments (orange), and the sequence closes with deposition of the uppermost limestone

- portion of Unit 2). Then as eruption proceeded, continuous explosions formed a tuff ring (Unit 2; Fig. 6) surrounding the crater by deposition from Surtseyan tephra jets and associated phenomena. The ring accumulated initially in a subaqueous environment, as demonstrated by the debris flow beds lower in the sequence, but gradually became emergent, as shown by the presence of accretionary lapilli and dune forms in the upper part of the tuff ring (Figs. 6, 12b). Surtseyan activity during the initial stages of eruptions in shallow subaqueous settings is widely accepted, as in the Fort a la Corne kimberlite field (Lefebvre and Kurszlaukis 2008), for example. Some of the Unit 2 beds may be the deposits of subaqueous sediment gravity flows that redeposited material displaced from oversteepened flanks of the initial tuff cone.
- 4) Continued eruption produced a steam-rich eruptive column that collapsed episodically to cause base surges, conducive to the formation of accretionary lapilli. This continued the vertical accretion of the ring through deposition from traction currents (sandwave beds; Fig. 6b). Subaerial emergence of the ring is also demonstrated by the paleosol in Unit 6 at the top of the sequence (beneath the Unit 7 marine limestone) at Monticelli.
  - 5) Isolation of the eruptive vent from the sea by build-up of the surrounding ring allowed drawdown of the water available for magma interaction, causing the eruptive centre to deepen (Fig. 12b-c). This differs from many Surtseyan eruptions where hydromagmatic explosions are succeeded by magmatic eruptions that build tephra cones, commonly by Strombolian activity (Lefebvre and Kurszlaukis 2008). Deepening of the eruptive site is demonstrated by the increased steepness of the country rock within the crater, with morphology that passed from saucer-shaped to vertical walls, whereas the appearance of mantle xenoliths (Scribano et al. 2009) in the uppermost layers of the tuff ring suggests a faster magma ascent rate (White 1991). This was accompanied by some widening of the crater as blocks of the limestone country rock, weakened by the explosive shocks, spalled or slid downwards into the crater, accompanied by breccia beds from the overlying rim. However, although the diatreme continued to deepen, we suggest that the maar crater reached its final width rather early in the history of the diatreme, as the decrease in bedrock slopes at an elevation about 100 m below the rim indicates that this was the floor of the maar. The limited availability of water for the continuing eruptions is evidenced by the abundance of tachylite in the Unit 3 breccias from within the diatreme. The depth of the diatreme root zone (*sensu* Lorenz and Kurszlaukis 2007) is unknown. The base of the CGD at 215 ma.s.l. exposes only nonbedded breccia, and it is impossible to properly estimate the depth to which the conduit extends by geologic field surveys alone.
  - 6) Water availability increased within the crater, either by a decreasing eruption rate or an increasing water supply to the crater, possibly due to breaching of the tuff ring (Fig. 12d). During this period of relative quiescence, we interpret the emergence of a centre of slow effusion on the diatreme floor that was submerged at sufficient depth to accommodate accumulation of a stratified cone of hyaloclastite (Unit 4) that was later buried by slumps of breccia higher within the diatreme (Fig. 12d-e).
  - 7) Late in its evolution, the CGD experienced the nonexplosive intrusion of dikes and plugs (Unit 5) of unvesiculated magma (Fig. 12f). These were emplaced within the breccia or, more often, at the contact between the diatreme breccias of Unit 3 and the country rock. Although they are exposed mainly along the western boundary of the diatreme, where the contact between Unit 3 and the country rock is very steep or vertical, it is likely that additional intrusions occurred in other portions of the diatreme, but are not now visible because they have been covered by slides of breccia, or recent colluvium. Although there is no direct control on the relative ages of the plugs and dikes or the hyaloclastite (e.g. cross-cutting relationships), both units are similarly nonvesicular, which could imply a similar age. Trends of decreasing volatile content (Collins et al. 2009; Gerlach 1980), effusion rate (Calvari et al. 1994, 2005a, b; Wadge 1981) and/or water availability (Calvari and Pinkerton 2004) have been described for many eruptions. Similar trends during the eruption of the CGD would explain many of the features of its development. Some of these intrusions (Unit 5) were emplaced within wet, unconsolidated deposits, as revealed by their glassy-quenched margins and peperitic textures. Potentially, the intrusion of the dikes caused local destabilization of the diatreme walls and prompted additional country rock and breccia collapses in the inner conduit.
  - 8) At some time after the end of the magmatic intrusions, the interior of the maar was water-filled, but was a quiet-water environment, as demonstrated by the fine lamination of the limestone beds of Unit 6 (Fig. 12f). Thus, the maar ring continued to provide a barrier to normal shallow marine wave and current energy. Evidence of a paleosol near the top of the Monticelli sequence (root traces) suggests that at least for some periods, the top of the ring was subaerially exposed. The ring itself was subject to erosion and periodic collapses that produced sediment gravity flows that were deposited rapidly in this lagoonal environment, as

shown by the abundance of soft-sediment and dewatering structures in these beds.

- 9) Ultimately, lowering of the ring by erosional processes, and/or local sea level rise re-established complete connection to the open ocean environment. Normal marine, shallow water carbonate deposition (Unit 7) resumed over the entire diatreme sequence.

#### Relationship to nearby volcanic features

As described by Calvari and Tanner (2000), the CGD is but one of a series of volcanic features exposed in the Iblei Mountains (Fig. 2a). A smaller diatreme complex occurs approximately 0.5 km to the south of the CGD (the so-called Cozzo Ferrante cone of Suinting and Schmincke 2009; Fig. 2a). Diatreme breccias identical to those in the CGD are partially exposed in outcrop, but the topography and extent of the exposures of the Cozzo Ferrante diatreme units suggest a much smaller pipe-like structure than the CGD, of about 0.7 km diameter. Further to the south, outcrops occur in the valley of the Anapo River (Fig. 2a) variously of intrusions, hyaloclastites and volcanoclastic breccias similar to those within the CGD (Suinting and Schmincke 2009).

While we recognize the widespread distribution of these volcanic and volcanoclastic units in the Anapo River Valley (Fig. 2a), we also note the significant differences in elevation between these outcrops and those of the CGD. As noted by Suinting and Schmincke (2009), for example, an outcrop of very finely laminated (papershale) diatomite probably represents a sequence of lagoonal sediments within a maar crater sheltered by a tephra ring 0.5 km to the south of the CGD, at Cozzo Ferrante. This outcrop is genetically similar to the laminated limestone of Unit 6 at CGD, but occurs at about 250 m lower elevation. Suinting and Schmincke (2009) prefer to explain all of the volcanic features in this area as the result of a single burst of volcanic activity, and therefore must describe the Anapo River Valley as a graben with >200 m vertical displacement to explain the stratigraphic offsets. Our interpretation differs in that we consider it more probable that there were distinct eruptive episodes, separated by quiescent intervals of shallow carbonate sedimentation.

We describe the formation of the CGD from a single eruption comprising many eruptive pulses, separated in space and time from other volcanic events in this region. This interpretation of a prolonged interval of regional activity is similar to the ~20 million year eruptive history interpreted for the Fort a la Corne kimberlite field during the Cretaceous (Lefebvre and Kurszlauskis 2008). Additionally, we exclude from our sequence of eruptive events the subaerial lava flow of Pliocene age (Carbone and Lentini

1981; Grasso et al. 1982, 1983) that Suinting and Schmincke (2009) considered contemporaneous with the emplacement of the CGD. This lava overlies the Unit 7 limestone and thus was emplaced well after the end of the CGD development.

#### Conclusions

The geologic evidence presented above demonstrates that the CGD is a maar-diatreme complex that formed on a submerged carbonate platform through hydromagmatic activity. The model for the evolution of this feature that we present illustrates how explosive pipe conduits may form in shallow submarine settings. The essential factor in this model is that the construction of the maar ring, which was initially by subaqueous debris flows or concentrated water-particle currents, and later by subaerial base surges, limited the flow of water into the eruptive vent, thus causing a drawdown of the explosive centre and deepening of the diatreme. Decreasing magma delivery rate caused a lessening of the explosive activity and allowed the vent to refill with water. Slow effusion in the deep water environment at the bottom of this vent caused the accumulation of hyaloclastite. Gradually the vent was filled by sediments that slid into the crater from the surroundings and by carbonate deposition in a quiet lagoon environment. Finally, open marine conditions were re-established, following the erosion of the maar ring and the rise of sea level. Although our model for the evolution of the CGD differs in some respects from the previously accepted models, we believe its validity is established by the field relationships demonstrated herein, and believe furthermore that our model might have applications to other maar-diatreme volcanoes in subaqueous environments.

**Acknowledgements** SC wishes to thank Vittorio Scribano, who introduced her to the problems concerning the emplacement of diatremes in the Iblean region and discussed about the meaning of xenoliths in diatremes, and Volker Lorenz for his precious hints and suggestions during a field survey. LT thanks the Faculty Research Committee of Le Moyne College for providing travel funds that made this collaboration possible. This paper has strongly benefitted from in-depth reviews, comments and suggestions by Bruce Kjarsgaard, Karoly Németh, and James White that greatly improved the clarity of the paper. The authors extend special thanks to James White for his careful editing of the manuscript and for generously offering help and advice during the review process.

#### References

- Aranda-Gómez JJ, Luhr JF (1996) Origin of the Joya Honda maar, San Luis Potosí, México. *J Volcanol Geotherm Res* 74:1–18

- Barberi F, Civetta L, Gasparini P, Innocenti F, Scandone R, Villari L (1974) Evolution of a section of the Africa-Europe plate boundary: paleomagnetic and volcanological evidence from Sicily. *Earth Planet Sci Lett* 22:123–132
- Basile C, Chauvet F (2009) Hydromagmatic eruption during the buildup of a Triassic carbonate platform (Oman Exotics): Eruptive style and associated deformations. *J Volcanol Geotherm Res* 183:84–96
- Bergh SG, Sigvaldason GE (1991) New field and laboratory evidence for the origin of hyaloclastite flows on seamount summits. *Bull Volcanol* 53:597–611
- Boxer GL, Lorenz V, Smith CB (1989) The geology and volcanology of the Argyle (AK1) lamproite diatreme, Western Australia. *Proc 4th Int Kimberlite Conference, Perth, Australia. Geol Soc Aust Spec Publ* 14:140–151
- Brand BD, Clarke AB (2009) The architecture, eruptive history, and evolution of the Table Rock Complex, Oregon: From a Surtseyan to an energetic maar eruption. *J Volcanol Geotherm Res* 180:203–224
- Calvari S, Pinkerton H (2004) Birth, growth and morphologic evolution of the "Laghetto" cinder cone during the 2001 Etna eruption. *J Volcanol Geotherm Res* 132:225–239. doi:10.1016/S0377-0273(03)00347-0
- Calvari S, Tanner LH (2000) Stages in the Sortino diatremes formation, eastern Sicily, Italy. *Eos Trans AGU* 81(48):1338
- Calvari S, Coltelli M, Neri M, Pompilio M, Scribano V (1994) The 1991–93 Etna eruption: chronology and geological observations. *Acta Vulcanol* 4:1–15
- Calvari S, Spampinato L, Lodato L, Harris AJL, Patrick MR, Dehn J, Burton MR, Andronico D (2005a) – Chronology and complex volcanic processes during the 2002–2003 flank eruption at Stromboli volcano (Italy) reconstructed from direct observations and surveys with a handheld thermal camera. *J Geophys Res* 110: B02201. doi:10.1029/2004JB003129
- Calvari S, Spampinato L, Lodato L, Harris AJL, Patrick MR, Dehn J, Burton MR, Andronico D (2005b) Correction to “Chronology and complex volcanic processes during the 2002–2003 flank eruption at Stromboli volcano (Italy) reconstructed from direct observations and surveys with a handheld thermal camera”. *J Geophys Res* 110:B02201. doi:10.1029/2005JB003723
- Carbone S, Lentini F (1981) Caratteri deposizionali delle vulcaniti del Miocene superiore negli Iblei (Sicilia sud-orientale). *Geol Romana* 20:79–101
- Cas RAF, Wright JV (1988) Volcanic successions, modern and ancient. Unwin Hyman, Oxford University Press, 528 pp
- Cas RAF, Landis CA, Fordyce RE (1989) A monogenetic, Surtla-type, Surtseyan volcano from the Eocene-Oligocene Waiareka-Deborah volcanics, Otago, New Zealand: a model. *Bull Volcanol* 51:281–298
- Cas RAF, Hayman P, Pittari A, Porrit L (2008a) Some major problems with existing models and terminology associated with kimberlite pipes from a volcanological perspective, and some suggestions. *J Volcanol Geotherm Res* 174:209–225
- Cas RAF, Porrit L, Pittari A, Hayman P (2008b) A new approach to kimberlite facies terminology using a revised general approach to the nomenclature of all volcanic rocks and deposits: Descriptive to genetic. *J Volcanol Geotherm Res* 174:226–240
- Catalano R, Di Stefano P, Sulli A, Vitale FP (1996) Paleogeography and structure of the central Mediterranean: Sicily and its offshore area. *Tectonophysics* 260:291–323
- Collins SJ, Pyle DM, Maclennan J (2009) Melt inclusions track pre-eruption storage and dehydration of magmas at Etna. *Geology* 37:571–574
- Cucuzza Silvestri S (1963) Proposal for a genetic classification of hyaloclastites. *Bull Volcanol* 25:315–322
- Dawson JB (1980) Kimberlites and their Xenoliths. Springer, Heidelberg
- Fisher RV, Schmincke H-U (1984) Pyroclastic Rocks. Springer, Heidelberg
- Fisher RV, Waters AC (1970) Base surge bed forms in maar volcanoes. *Am J Sci* 268:157–280
- Gerlach TM (1980) Evaluation of volcanic gas analysis from Surtsey volcano, Iceland 1964–1967. *J Volcanol Geotherm Res* 8:191–198
- Gilbert JS, Lane SJ (1994) The origin of accretionary lapilli. *Bull Volcanol* 56:398–411
- Grasso M, Lentini F, Pedley HM (1982) Late Tortonian-Lower Messinian (Miocene) palaeogeography of SE Sicily: information from two new formations of the Sortino Group. *Sedim Geol* 32:279–300
- Grasso M, Lentini F, Nairn AEM, Vigliotti L (1983) A geological and paleomagnetic study of the Hyblean volcanic rocks, Sicily. *Tectonophysics* 98:271–295
- Hearn BC Jr (1968) Diatremes with kimberlitic affinities in north-central Montana. *Science* 159:622–625
- Hine AC (1977) Lily Bank, Bahamas: history of an active oolite sand shoal. *J Sedim Petrol* 47(4):1554–1581
- Kienle J, Kyle PR, Self S, Motyka RJ, Lorenz V (1980) Ukinrek Maars, Alaska, I. April, 1997, eruption sequence, petrology and tectonic setting. *J Volcanol Geotherm Res* 7:11–37
- Kokelaar BP (1983) The mechanism of Surtseyan volcanism. *J Geol Soc Lond* 140:939–944
- Kokelaar P, Durant GP (1983) The submarine eruption and erosion of Surtla (Surtsey), Iceland. *J Volcanol Geotherm Res* 19:239–246
- Kurszlauskis S, Lorenz V (2008) Formation of “Tuffistic” Kimberlites by phreatomagmatic processes. *J Volcanol Geotherm Res* 174:68–80
- Lefebvre N, Kurszlauskis S (2008) Contrasting eruption styles of the 147 Kimberlite, Fort à la Corne, Saskatchewan, Canada. *J Volcanol Geotherm Res* 174:171–185
- Lorenz V (1973) On the Formation of Maars. *Bull Volcanol* 37:183–204
- Lorenz V (1985) Maars and diatremes of phreatomagmatic origin: a review. *Trans Geol Soc SA* 88:459–470
- Lorenz V (1986) On the growth of maars and diatremes and its relevance to the formation of tuff rings. *Bull Volcanol* 48:265–274
- Lorenz V (2007) Syn- and post-eruptive hazards of maar-diatreme volcanoes. *J Volcanol Geotherm Res* 159:285–312
- Lorenz V, Kurszlauskis S (2007) Root zone processes in the phreatomagmatic pipe emplacement model and consequences for the evolution of maar-diatreme volcanoes. *J Volcanol Geotherm Res* 159:4–32
- Lorenz V, Zimanowski B, Büttner R (2002) On the formation of deep-seated subterranean peperite-like magma-sediment mixtures. *J Volcanol Geotherm Res* 114:107–118
- Martin U, Németh K (2005) Eruptive and depositional history of a Pliocene tuff ring that developed in a fluvio-lacustrine basin: Kissomlyó volcano (western Hungary). *J Volcanol Geotherm Res* 147:342–356
- Martin U, Breiterkreuz C, Egenho S, Enos P, Jansa L (2004) Shallow-marine phreatomagmatic eruptions through a semi-solidified carbonate platform (ODP Leg 144, Site 878, Early Cretaceous, MIT Guyot, West Pacific). *Mar Geol* 204:251–272
- McClintock MK, White JDL (2006) Large-volume phreatomagmatic vent complex at Coombs Hills, Antarctica records wet, explosive initiation of flood basalt volcanism in the Ferrar LIP. *Bull Volcanol* 68:215–239
- Nemec W, Steel RJ (1984) Alluvial and coastal conglomerates: their significant features and some comments on gravelly mass-flow deposits. In: Koster LH and Steel RJ (eds) *Sedimentology of Gravels and Conglomerates*, Can Soc Petroleum Geol Memoir 10:1–31
- Németh K, White CM (2009) Intra-vent peperites related to the phreatomagmatic 71 Gulch Volcano, western Snake River Plain

- volcanic field, Idaho (USA). *J Volcanol Geotherm Res* 183:30–41
- Németh K, Goth K, Martin U, Csillag G, Suhr P (2008) Reconstructing paleoenvironment, eruption mechanism and paleomorphology of the Pliocene Pula maar, (Hungary). *J Volcanol Geotherm Res* 177:441–456
- Newell ND, Purdy EG, Imbrie J (1960) Bahamian oolitic sand. *J Geol* 68:481–497
- Pedley HM, Grasso M (1991) Sea-level change around the margins of the Catania-Gela Trough and Hyblean Plateau, southeast Sicily (African-European plate convergence zone): a problem of Plio-Quaternary plate buoyancy? *Spec Pub Int Assoc Sedimentol* 12:461–464
- Rittmann A (1973) Lave a pillow ed ialoclastiti. *Rend Soc Ital Miner Petrol* 29:397–412
- Ross P-S, White JDL (2006) Debris jets in continental phreatomagmatic volcanoes: a field study of their subterranean deposits in the Coombs Hills vent complex, Antarctica. *J Volcanol Geotherm Res* 149:62–84
- Ross P-S, White JDL, Zimanowski B, Büttner R (2008) Multiphase flow above explosion sites in debris-filled volcanic vents: Insights from analogue experiments. *J Volcanol Geotherm Res* 178:104–112
- Scarfì L, Giampiccolo E, Musumeci C, Patané D, Zhang H (2007) New insights on 3D crustal structure in southeastern Sicily (Italy) and tectonic implications from an adaptive mesh seismic tomography. *Phys Earth Planet Int* 161:74–85
- Schipper CI, White JDL, Houghton BF (2010) Syn- and post-fragmentation textures in submarine pyroclasts from Lo'ihi Seamount, Hawai'i. *J Volcanol Geotherm Res* 191:93–106
- Schmincke HU, Behncke B, Grasso M, Raffi S (1997) Evolution of the northwestern Iblean Mountains, Sicily: uplift, Pliocene/Pleistocene sea-level changes, paleoenvironment, and volcanism. *Geol Rundsch* 86:637–669
- Schmincke HU, Grasso M, Sturiale G, Suiting I (2004) The Neogene volcanism of the northern Monti Iblei in south-eastern Sicily. 32nd Int Geol Congress, Florence, Italy, Field Trip Guide B30, 2:30–36
- Schumacher R, Schmincke HU (1995) Models for the origin of accretionary lapilli. *Bull Volcanol* 56:626–639
- Scribano V, Viccaro M, Cristofolini R, Ottolini L (2009) Metasomatic events recorded in ultramafic xenoliths from the Hyblean area (Southeastern Sicily, Italy). *Mineral Petrol* 95:235–250
- Self S, Kienle J, Huot JP (1980) Ukinrek maars, Alaska, II. Deposits and formation of the 1977 craters. *J Volcanol Geotherm Res* 7:39–65
- Skilling IP, White JDL, McPhie J (2002) Peperite: a review of magma-sediment mingling. *J Volcanol Geotherm Res* 114:1–17
- Skinner EMV, Marsh JS (2004) Distinct kimberlite pipe classes with contrasting eruption processes. *Lithos* 76:183–200
- Smith TL, Batiza R (1989) New field and laboratory evidence for the origin of hyaloclastite flows on seamount summits. *Bull Volcanol* 51:96–114
- Sohn JK (1995) Geology of Tok Island, Korea – Eruptive and depositional processes of a shoaling to emergent island volcano. *Bull Volcanol* 56:660–674
- Sohn YK, Park JB, Khim BK, Park KH, Koh GW (2002) Stratigraphy, petrochemistry and Quaternary depositional record of the Songaksan tuff ring, Jeju Island, Korea. *J Volcanol Geotherm Res* 119:1–20
- Sohn YK, Park KH, Yoon SH (2008) rimary versus secondary and subaerial versus submarine hydrovolcanic deposits in the subsurface of Jeju Island, Korea. *Sedimentology* 55:899–924
- Stoppa F, Principe C (1997) Eruption style and petrology of a new carbonatitic suite from the Mt. Vulture (Southern Italy): the Monticchio Lakes Formation. *J Volcanol Geotherm Res* 80:137–153
- Suiting I, Schmincke H-U (2009) Internal vs. external forcing in shallow marine diatreme formation: A case study from the Iblean Mountains (SE-Sicily, Central Mediterranean). *J Volcanol Geotherm Res* 186:361–378
- Tanner LH, Calvari S (1999) Facies analysis and depositional mechanism of hydroclastite breccias, Acicastello, eastern Sicily. *Sedim Geol* 129:127–141
- Tonarini S, D'Orazio M, Armienti P, Innocenti F, Scribano V (1996) Geochemical features of Eastern Sicily lithosphere as probed by Hyblean xenoliths and lavas. *Eur J Miner* 8:1153–1173
- Wadge G (1981) The variation of magma discharge during basaltic eruptions. *J Volcanol Geotherm Res* 11:139–168
- White JDL (1991) Maar-diatreme phreatomagmatism at Hopi Buttes, Navajo Nation (Arizona), USA. *Bull Volcanol* 53:239–258
- White JDL (1996) Pre-emergent construction of a lacustrine basaltic volcano, Pahvant Butte, Utah (USA). *Bull Volcanol* 58:249–262
- White JDL (2000) Maars, maar-rim deposits and diatremes – an overview of volcanism and sedimentation in the Hopi Buttes volcanic field, Arizona, USA. *Terra Nostra* 6:500–505, Int Maar Conference, Daun/Vulkaneifel, Extended Abs
- White JDL, Houghton BF (2000) Surtseyan and related eruptions. In: Sigurdsson H, Houghton B, McNutt S, Rymer H, Stix J (eds) *Encyclopedia of Volcanoes*. Academic, New York, pp 495–512
- White JDL, Houghton BF (2006) Primary volcanoclastic rocks. *Geology* 34:677–680
- White JDL, McPhie J, Skilling I (2000) Peperite: a useful genetic term. *Bull Volcanol* 62:65–66
- Wilson L, Head JW (2007) An integrated model of kimberlite ascent and eruption. *Nature* 447:53–57
- Wohletz KH (1986) Explosive magma-water interactions: Thermodynamics, explosion mechanisms, and field studies. *Bull Volcanol* 48:245–264
- Yellin-Dror A, Grasso M, Ben-Avraham Z, Tibor G (1997) The subsidence history of the northern Hyblean plateau margin, southeastern Sicily. *Tectonophysics* 282:277–289